Simulation And Analysis Of A Rotary-Inverted Pendulum Utilizing Lagrangian Equation Of Motion

Imad burhan Kadhim
Electronic Department, Kirkuk Technical Institute, Northern Technical University, Kirkuk, Iraq
imadburhan86@ntu.edu.iq

ABSTRACT

Detailed Inverted pendulum systems' mechanical configurations show a great deal of variation. In order to better understand the dynamics of the commonly-referred-to as the "Rotary inverted system," an enlarged unstable Rotary planer inverted pendulum configuration, this research employs mathematical concepts. Pinned connections are often used to securely attach the inverted pendulum to the rotating actuation base in planar pendulums. The analysis of a Rotary-inverted pendulum is presented in this study to aid in the progress of underactuated robotic system development. This design is particularly noteworthy because to its capacity to precisely emulate the equilibrium seen while holding a broomstick, which is accomplished by considering the revolute joints of the elbow and shoulder. The dynamical equation for the Rotary-inverted pendulum may be formulated by using the Lagrangian equation of motion. Because of its flexibility and user-friendliness, the MATLAB programming language and environment is widely used in the scientific and technical fields. The accuracy of a nonlinear computational model of a system may be checked by simulation in Simulink.

Keywords: Lagrangian, Rotary-Inverted Pendulum, Broomstick.

1 INTRODUCTION

Attempting to stabilize a nonlinear inverted pendulum is a significant problem for modern control theory. The complex structure of the system's modeling, stabilization, and trajectory monitoring makes this a very difficult problem to solve. Given the relevance of pendulum balancing principles to the stabilization of human transporter Segways and humanoid robots, it is not surprising that they have been applied to a wide variety of fields, including rocket thrusters, aviation systems, maritime systems, and space vehicles[1][2]. The careful consideration of actuation technologies and the number of degrees of freedom has great significance in the design and development of an inverted pendulum within the field of mechanical engineering. Both linear and rotary mechanisms may be used as actuation techniques. There are two degrees of freedom (DOF) that may be adjusted in systems that use inverted pendulums, such as the rotary inverted pendulum and cart inverted pendulum the position of the base and the orientation of the pendulum. In the context of an inverted pendulum system, linkage between mechanical a pendulum in oscillatory motion and a cart undergoing rotational movement a pin joint is used [3][4][5].

The cart, propelled by its motor, is thus able to rotate inside the horizontal plane. The RIP consists of a main arm, a main pendulum, and a main motor. Using a pin joint mechanism, the inverted pendulum of the Rotary system may swing freely in the vertical direction. The pendulum is securely attached to one arm, and the motor shaft is solidly secured to the other. The use of an inverted pendulum as a mechanical system Several design options may be used to augment flexibility, such as incorporating multi-dimensional movement capabilities into the base or integrating additional pendulum attachments into the design. When the base has the capacity to move in two separate directions, it requires the existence of two degrees of freedom [6][7][8].

The use of this technology has resulted in the establishment of a horizontal plane. The term in question is referred to as (PIPS). It is possible to employ rotational-rotational action, linear-linear actuation, or a mix of the two using the planar inverted pendulum system's mechanical configurations. There is a lack of knowledge on the design of such systems, with just a few articles addressing the issue, despite the fact that RIP and cart inverted pendulum systems have been designed and realized. The inverted cart pendulum system

Manuscript received on: 28.12.2023
Accepted on: 25.01.2024
Published on: 30.01.2024
Issue DOI: doi.org/10.52688/22

was modeled using Newtonian principles. The dynamics of the spinning inverted pendulum, were characterized using the Lagrangian equation of motion, which accounts for its nonlinear behavior. The Furuta pendulum was thoroughly elucidated by the aforementioned individual. The mechanical design of the Furuta pendulum was created using the Lagrangian equation of motion and the SolidWorks software. It was the goal of this work to develop a mathematical model of a dual-axis inverted pendulum system that takes into consideration the dynamics of the actuator while maintaining a commitment to the principle of energy conservation. Researchers have successfully developed a robot with a limited range of motion, consisting of just two degrees of freedom. The paper in which the researchers provided a comprehensive account of their findings was identified. The pendulum was affixed to the SCARA robot using either decoupled or weakly coupled connections. Linear and nonlinear control methodologies were used to maintain the vertical ascension of an inverted pendulum. This paper elucidates the procedure for eliminating the limit cycle of the Furuta pendulum [9][10]. Few writers have tried to imitate the dynamics of the linear-inverted pendulum system, according to a thorough review of the current literature. In this study, we provide a novel approach to RIP (Rotary Inverted Pendulum) system modelling. Previous methods of connecting the pendulum to its rotary-planar actuation base used unconnected links; this approach is different. A pin joint mechanism for the RIP system and nonlinear computer modelling approaches make up the technology being discussed. There has been a lot of buzz in the world of underactuated robotic systems research about the inverted pendulum arrangement, which is a planer with an inverted pendulum. Due to its striking similarity to the complex equilibrium seen when holding a broomstick, the design being considered is of particular importance. This is made possible since the model's elbow and shoulder joints are modelled as revolute joints. The model is built with the help of the Lagrangian mathematical framework. Numerical simulation with MATLAB Simulink was used to verify the mathematical model of the nonlinear system [11].

2 THE DESIGN OF THE REVOLVING INVERTED PENDULUM

Figure 1 is a schematic showing how a rotary planer may be used to make an inverted pendulum. Arm 1, Arm 2, and Pendulum 3 are crucial constituents of the overall framework. The horizontal motion of the DC motor is facilitated by the connection between the shaft and arm 1. The use of a servo motor enables the application of torque at the revolute joint that connects the first and second arms, therefore facilitating the rotation of the robot within the horizontal plane. Arm 2 is connected to the pendulum by a pin joint, allowing for unrestricted swinging motion within the vertical plane [12][13][14]. Figure 2 displays three angles, each corresponding to one of the arms. Angle q_1 represents the angular separation between the first and second arms, measured at a point that has been randomly selected. The angle q_2 represents the angular displacement between the second arm and the first arm. The angular displacement of the pendulum is denoted by the variable q_3. Negative angular displacements do not occur during a rotation in the clockwise direction. m_1, m_2, and m_3 stand for the relative masses of the first two arms, the pendulum, and the third component, the mass balance. The two higher extremities demonstrate the highest magnitude in terms of length, whereas the pendulum is characterized by measurements represented as L_2 and L_3. The variables I_1, I_2, and I_3 denote the angular displacements of the first arm, second arm, and pendulum, respectively [15]. These symbols correspond to the distances measured from the pivot points of the corresponding arms.

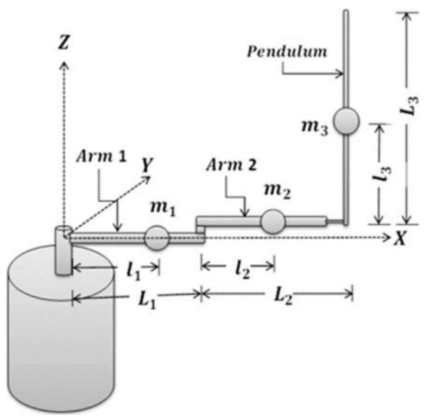

Figure 1. The Quanser With the Inverted Pendulum.

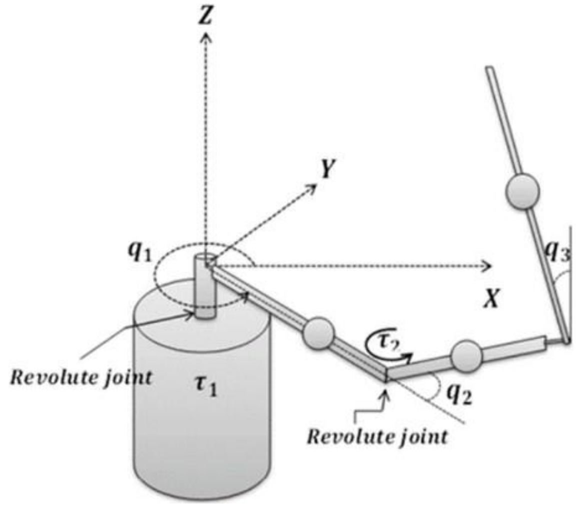

Figure 2. The quanser-inverted pendulum makes use of both torque applications and relative joint-angle motions.

Torque one and torque two, denoted in reference to the respective electric motors generating them, are used for the purpose of actuating arms 1 and 2. The pendulum's direction of swing may be manipulated by deactivating arm 2. The symbols l_1 and l_2 are used to denote the moment of inertia tensors for the first and second arms, respectively. Similarly, the symbol l_3 denotes the moment of inertia tensor with respect to the center of mass. The damping coefficients associated with the joint are represented by the symbols b1, b2, and b3.

3 QUANSER INVERTED PENDULUM

Being a three-DOF system, the inverted Rotary pendulum is governed by three distinct sets of Lagrangian equations of motion.

$$\frac{d}{dt}\left(\frac{\partial L}{\partial \dot{q}_1}\right)-\frac{\partial L}{\partial q_1}=\tau_1-b_1\dot{q}_1 \tag{1}$$

$$\frac{d}{dt}\left(\frac{\partial L}{\partial \dot{q}_2}\right)-\frac{\partial L}{\partial q_2}=\tau_2-b_2\dot{q}_2 \tag{2}$$

$$\frac{d}{dt}\left(\frac{\partial L}{\partial \dot{q}_3}\right)-\frac{\partial L}{\partial q_3}=-b_3\dot{q}_3 \tag{3}$$

The distinction between kinetic and potential energy may be elucidated, using the Lagrangian of the system denoted as $\mathcal{L}$.

$$L = E_k - E_p \tag{4}$$

The kinetic energy inside an inverted pendulum system is often indicated as E_{k3}, whilst the potential energy is symbolized as E_p. The determination of the total potential energy is contingent upon the collective contributions of both kinetic energy (E_k) and potential energy (E_p). The aggregate kinetic energy is equal to the combined energies linked to the motion of two appendages and a pendulum. Furthermore, the total potential energy, represented as E_p, is equivalent to the aggregate of all three energy components. It is hypothesized that the potential energy of Arms 1 and 2 is negligible as a result of their motion along a horizontal plane.

$$E_{p1} = E_{p2} = 0 \tag{5}$$

The computation of the pendulum's potential energy may be facilitated by referring to Figure 3.

$$E_{p3} = m_3 g l_3 \left(\cos(q_3) - 1\right) \tag{6}$$

The total potential energy of arm 1 is identical to, if only because we assume that arms 1 and 2 have the same amount of potential energy.

$$E_p = E_{p1} + E_{p2} + E_{p3} \tag{7}$$

The kinetic energy associated with Arm 1 is.

$$E_{k1} = \frac{1}{2} m_1 v_1^T v_1 + \frac{1}{2} J_1 \dot{q}_1^2 \tag{8}$$

Consequently, it is important to thoroughly investigate the kinematics of the subject in order to achieve comprehensiveness. The diagram in Figure 3 shows how the weight distribution along Arm 1 is dependent on its location.

$$O_1 = \left[x_1, y_1, z_1\right]^T \tag{9}$$

An example of a free body diagram with well-defined variable meanings is shown in Figure 3(a), where the variables a and b are given meaningful labels.

$$x_1 = l_1 \cos\left(q_1\right), y_1 = l_1 \sin\left(q_1\right), z_1 = 0$$

Stated otherwise, it might be posited that

$$v_1 = \left[\dot{x}_1, \dot{y}_1, \dot{z}_1\right]^T \tag{10}$$

Being

$$\dot{x}_1 = -\dot{q}_1 l_1 \sin\left(q_1\right), \dot{y}_1 = \dot{q}_1 l_1 \cos\left(q_1\right), \dot{z}_1 = 0$$

The subsequent outcome is seen when equation (10) is substituted for equation (8), followed by the rearrangement of the expression.

$$E_{k1} = \frac{1}{2} m_1 l_1^2 \dot{q}_1^2 + \frac{1}{2} J_1 \dot{q}_1^2 \tag{11}$$

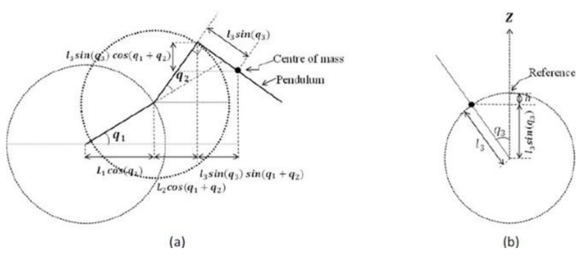

Figure 3. The rotating graphic is used to analyze a free-body inverted pendulum from a horizontal perspective. A vertical projectile is assumed.

The determination of the kinetic energy of the second arm and the pendulum may be achieved by using the aforementioned variables, which are denoted in a manner similar to the previously described approach. The individuals in question were characterized using the following terms:

$$E_{k2} = \frac{1}{2} m_2 \begin{bmatrix} L_1^2 \dot{q}_1^2 + l_2^2 \left(\dot{q}_1 + \dot{q}_2\right)^2 + \\ 2 L_1 l_2 \dot{q}_1 \left(\dot{q}_1 + \dot{q}_2\right) \cos\left(q_2\right) \end{bmatrix} + \frac{1}{2} J_2 \left(\dot{q}_1 + \dot{q}_2\right)^2 \tag{12}$$

$$E_{k3} = \frac{1}{2} J_3 \dot{q}_3^2 + \frac{1}{2} m_3 \begin{bmatrix} L_1^2 \dot{q}_1^2 + l_3^2 \dot{q}_3^2 + \left(\dot{q}_1 + \dot{q}_2\right)^2 l_3^2 \sin^2\left(q_3\right) + \left(\dot{q}_1 + \dot{q}_2\right)^2 L_2^2 \\ -2 \dot{q}_3 \left(\dot{q}_1 + \dot{q}_2\right) l_3 L_2 \cos\left(q_3\right) - 2 \dot{q}_1 \dot{q}_3 \cos\left(q_2\right)\cos\left(q_3\right) \\ +2 \dot{q}_1 \left(\dot{q}_1 + \dot{q}_2\right) l_3 L_1 \sin\left(q_2\right) \sin\left(q_3\right) + \\ 2 \dot{q}_1 \left(\dot{q}_1 + \dot{q}_2\right) L_1 L_2 \cos\left(q_2\right) \end{bmatrix}$$

When the energy of the first and second arms, as well as the pendulum, are summed together, the sum is equal to the kinetic energy of the whole system.

$$E_k = E_{k1} + E_{k2} + E_{k3} \tag{14}$$

The equation represented as (14) may be derived by substituting the previously specified values for kinetic and potential energy into the formula and then simplifying it.

$$\begin{aligned} \mathrm{L} = {} & \frac{1}{2} \dot{q}_1^2 \left[J_1 + m_1 l_1^2\right] + \frac{1}{2} J_2 \left(\dot{q}_1 + \dot{q}_2\right)^2 + \frac{1}{2} m_2 \\ & \begin{bmatrix} L_1^2 \dot{q}_1^2 + l_2^2 \left(\dot{q}_1 + \dot{q}_2\right)^2 \\ +2 L_1 l_2 \dot{q}_1 \left(\dot{q}_1 + \dot{q}_2\right) \cos\left(q_2\right) \end{bmatrix} \\ & + \frac{1}{2} J_3 \dot{q}_3^2 + \frac{1}{2} m_3 \\ & \begin{bmatrix} L_1^2 \dot{q}_1^2 + l_3^2 \dot{q}_3^2 + \left(\dot{q}_1 + \dot{q}_2\right)^2 l_3^2 \sin\left(q_3\right) + \left(\dot{q}_1 + \dot{q}_2\right)^2 L_2^2 \\ -2 \dot{q}_3 \left(\dot{q}_1 + \dot{q}_2\right) l_3 L_2 \cos\left(q_3\right) - 2 \dot{q}_1 \dot{q}_3 \cos\left(q_2\right) \cos\left(q_3\right) \\ +2 \dot{q}_1 \left(\dot{q}_1 + \dot{q}_2\right) l_3 L_1 \sin\left(q_2\right) \sin\left(q_3\right) \\ +2 \dot{q}_1 \left(\dot{q}_1 + \dot{q}_2\right) L_1 L_2 \cos\left(q_2\right) \end{bmatrix} \\ & - m_3 g l_3 \left(\cos\left(q_3\right) - 1\right) \end{aligned} \quad (15$$

The computation of the Euler-Lagrange terms is performed, followed by their insertion into equations 1 through 3. Eventually, a set of simultaneous differential equations will be formulated as a result of this procedure.

$$\begin{bmatrix} \left(M_{11}\ddot{q}_1 + M_{12}\ddot{q}_2 + M_{13}\ddot{q}_3 + C_{11}\dot{q}_1 + C_{12}\dot{q}_2 + C_{13}\dot{q}_3 + G_1 + F_{v1}\right) \\ \left(M_{21}\ddot{q}_1 + M_{22}\ddot{q}_2 + M_{23}\ddot{q}_3 + C_{21}\dot{q}_1 + C_{22}\dot{q}_2 + C_{23}\dot{q}_3 + G_2 + F_{v2}\right) \\ \left(M_{31}\ddot{q}_1 + M_{32}\ddot{q}_2 + M_{33}\ddot{q}_3 + C_{31}\dot{q}_1 + C_{32}\dot{q}_2 + C_{33}\dot{q}_3 + G_3 + F_{v3}\right) \end{bmatrix} = \begin{bmatrix} \tau_1 \\ \tau_2 \\ 0 \end{bmatrix}$$

$$M_{11}=J_1+J_2+m_1l_1^2+m_2L_1^2+m_2l_2^2+m_3L_1^2+m_3L_2^2+2m_2L_1L_2\cos(q_2)+m_3l_3^2\sin^2(q_3)$$
$$+2m_3l_3L_1\sin(q_2)\sin(q_3)+2m_3L_1L_2\cos(q_2),$$
$$M_{12}=J_2+m_2l_2^2+m_3L_2^2+m_2L_1l_2\cos(q_2)+m_3l_3L_1\sin(q_2)\sin(q_3)+m_3L_1L_2\cos(q_2)$$
$$+m_3l_3^2\sin^2(q_3),$$
$$M_{13}=-m_3L_2l_3\cos(q_3)-m_3l_3L_1\cos(q_2)\cos(q_3),M_{21}=M_{12},$$
$$M_{22}=J_2+m_2l_2^2+m_3L_2^2+m_3l_3^2\sin^2(q_3),$$
$$M_{23}=-m_3L_2l_3\cos(q_3),$$
$$M_{31}=M_{13},M_{32}=M_{23},M_{33}=J_3+m_3l_3^2,$$
$$C_{11}=-2\dot{q}_2m_2L_1l_2\sin(q_2)+\dot{q}_3m_3l_3^2\sin(2q_2)+2\dot{q}_2m_3l_3L_1\cos(q_2)\sin(q_3)$$
$$+2\dot{q}_3m_3l_3L_1\sin(q_2)\cos(q_3)-2\dot{q}_2m_3L_1L_2\sin(q_2),$$
$$C_{12}=-\dot{q}_2m_2L_1l_2\sin(q_2)+\dot{q}_3m_3l_3^2\sin(2q_3)-2\dot{q}_3m_3l_3L_1\sin(q_2)\cos(q_3)$$
$$+\dot{q}_2m_3l_3L_1\cos(q_2)\sin(q_3)-\dot{q}_2m_3L_1L_2\sin(q_2),$$
$$C_{13}=\dot{q}_3m_3L_2l_3\sin(q_3)+\dot{q}_3m_3l_3L_1\sin(q_3)\cos(q_2),$$
$$C_{21}=-3\dot{q}_2m_2L_1l_2\sin(q_2)+\dot{q}_3m_3l_3^2\sin(2q_3)-2\dot{q}_1m_2L_1l_2\sin(q_2)$$
$$-\dot{q}_1m_3l_3L_1\sin(q_3)\cos(q_2)+\dot{q}_1m_3L_1L_2\sin(q_2),$$
$$C_{22}=\dot{q}_3m_3l_3^2\sin(2q_3),C_{23}=\dot{q}_3m_3l_3L_2\sin(q_3),$$
$$C_{31}=\dot{q}_3m_3l_3L_1\cos(q_2)\cos(q_3)+\frac{1}{2}\dot{q}_1m_3l_3^2\sin(2q_3)+\dot{q}_2m_3l_3^2\sin(2q_2)$$
$$-\dot{q}_1m_3l_3L_1\sin(q_3)\cos(q_2)-\dot{q}_1m_3l_3L_1\sin(q_3)\sin(q_2),$$
$$G_1=0,G_2=0,G_3=-m_3gl_3\sin(q_3),F_{v1}=b_1\dot{q}_1,F_{v2}=b_2\dot{q}_2,F_{v3}=b_3\dot{q}_3.$$

Speculation about the rotating motion of an inverted pendulum. For modeling purposes, the nonlinear dynamical equation (16) of the Rotary inverted pendulum system was developed in MATLAB. The estimation of key parameters, namely q_1 , q_2, and q_2, will be conducted via the use of an inverted pendulum simulation. The data derived from this simulation will be used to improve the understanding of the behavior of the system. Table 1 displays the estimated and observed values for the parameters of the Rotary Inverted Pendulum (RIP) system, which have been obtained based on its fundamental properties. The availability of this experimental set-up is often seen in laboratory settings.

Table 1. Parameter estimates for a revolving inverted pendulum system

Symbol	Value	Units
L_1	0.1318	M
L_2	0.09312	M
L_3	0.49	M
l_1	$L_1/2$	M
l_2	$L_2/2$	M
l_3	$L_3/2$	M
m_1	0.048	Kg
m_2	0.03835	Kg
m_3	0.030	Kg
J_1	1.065×10^{-4}	$Kg.m^2$
J_2	3.0270×10^{-5}	$Kg.m^2$
J_3	9.8450×10^{-4}	$Kg.m^2$
b_1	0.00019	Nms
b_2	0.00016	Nms
b_3	0.00025	Nms
g	9.81	m/s^2

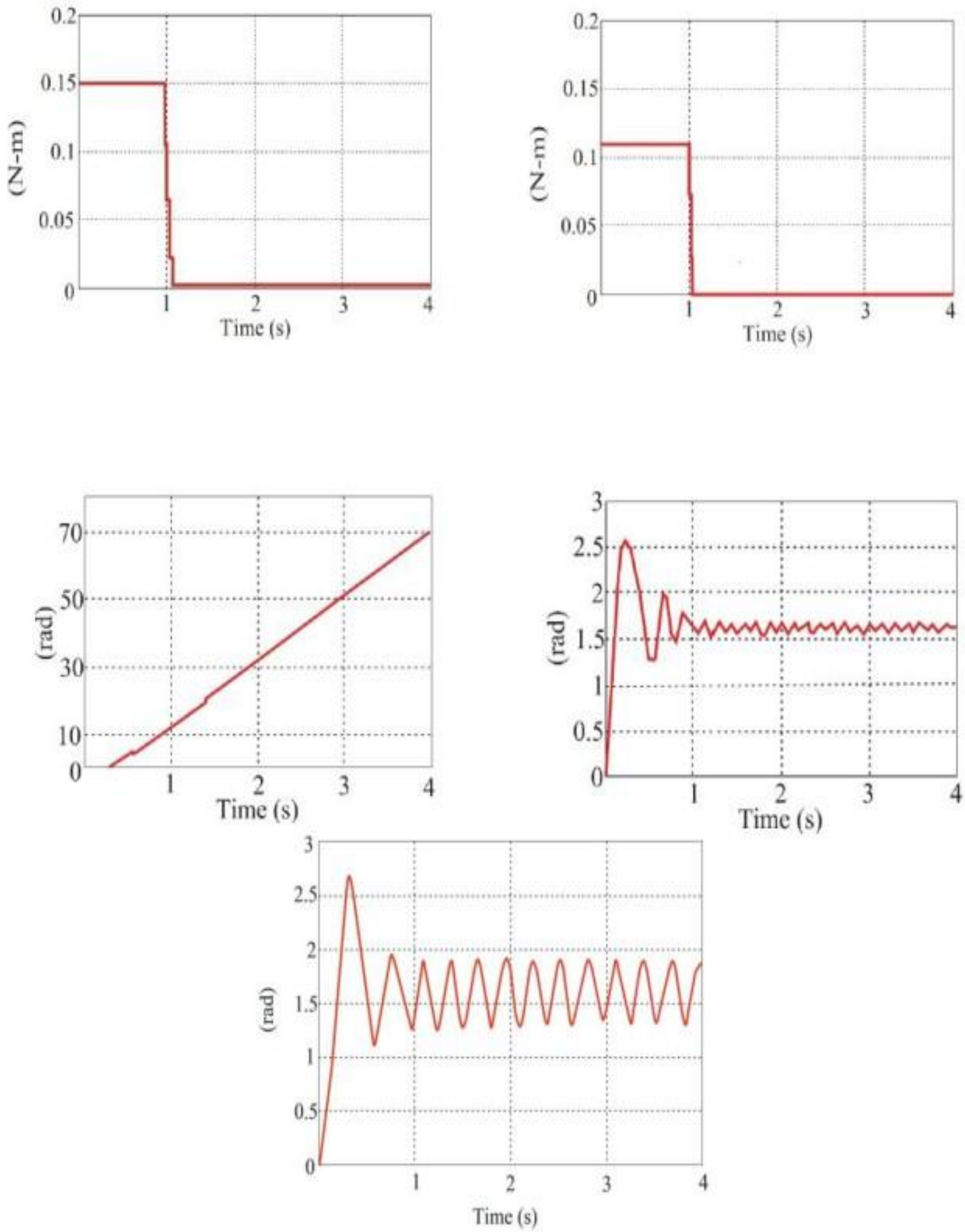

Figure 4. Response of an inverted pendulum that rotates in a plane

The pendulum shown in Figure 4 is seen by numerical simulation, with its initial position aligned with the 0 radian line, which corresponds to a vertical upward orientation. For the first second, a torque of 0.15 Nm is applied to actuating arm 1, and then for the second second, a torque of 0.13 Nm is applied to actuating arm 2. When external force is applied to the arms of the pendulum, it will deviate from its initial vertical position by about 1.57 percent of its original length. Figure 4 provides a comprehensive analysis of the simulation's outcomes. The rotational motion of arms 1 and 2 inside the provided system would be greatly helped by a diagram depicting this motion. The application of torque to the primary and secondary arms causes the corresponding motions to be realized. In Image 4, the radian angle is about 1.57. This deviation from the vertical equilibrium position of the pendulum is attributed to the lack of a stabilizing mechanism.

4. CONCLUSIONS

The present research provides a thorough evaluation and simulation of a rotary planer system that makes use of an inverted pendulum. Establishing the Lagrangian equation of motion is the first step in this investigation, followed by the development of computational models. The computer model of the pendulum and its accessories used geometric projections in the horizontal and vertical planes to show the precise locations of the pendulum and its components. The use of the MATLAB-Simulink software package has facilitated the construction of a nonlinear model and the subsequent execution of simulations. This research elucidates the potential success of combining the planar inverted pendulum system with the Rotary inverted pendulum system, as shown by the use of a computer model.

References

[1] Grasser, F., D'arrigo, A., Colombi, S., & Rufer, A. C. (2002). JOE: a mobile, inverted pendulum. IEEE

[2] Anderson, C. W. (1989). Learning to control an inverted pendulum using neural networks. IEEE Control Systems Magazine, 9(3), 31-37.

[3] Boubaker, O. (2013). The inverted pendulum benchmark in nonlinear control theory: a survey. International Journal of Advanced Robotic Systems, 10(5), 233.

[4] Huang, S. J., & Huang, C. L. (2000). Control of an inverted pendulum using grey prediction model. IEEE transactions on industry applications, 36(2), 452-458.

[5] Kuo, A. D., Donelan, J. M., & Ruina, A. (2005). Energetic consequences of walking like an inverted pendulum: step-to-step transitions. Exercise and sport sciences reviews, 33(2), 88-97.

[6] Boubaker, O. (2012, July). The inverted pendulum: A fundamental benchmark in control theory and robotics. In International conference on education and e-learning innovations (pp. 1-6). IEEE.

[7] Milton, J., Cabrera, J. L., Ohira, T., Tajima, S., Tonosaki, Y., Eurich, C. W., & Campbell, S. A. (2009). The time-delayed inverted pendulum: implications for human balance control. Chaos: An Interdisciplinary Journal of Nonlinear Science, 19(2).

[8] Wang, J. J. (2011). Simulation studies of inverted pendulum based on PID controllers. Simulation Modelling Practice and Theory, 19(1), 440-449.

[9] Kafetzis, I., & Moysis, L. (2017). Inverted Pendulum: A system with innumerable applications. School of Mathematical Sciences.

[10] Kuo, A. D. (2007). The six determinants of gait and the inverted pendulum analogy: A dynamic walking perspective. Human movement science, 26(4), 617-656.

[11] Furuta, K., Okutani, T., & Sone, H. (1978). Computer control of a double inverted pendulum. Computers & Electrical Engineering, 5(1), 67-84.

[12] Li, Z., Yang, C., & Fan, L. (2012). Advanced control of wheeled inverted pendulum systems. Springer Science & Business Media.

[13] Furuta, K., Yamakita, M., & Kobayashi, S. (1991, October). Swing up control of inverted pendulum. In IECON (Vol. 91, pp. 2193-2198).

[14] Kajiwara, H., Apkarian, P., & Gahinet, P. (1999). LPV techniques for control of an inverted pendulum. IEEE Control Systems Magazine, 19(1), 44-54.

[15] Stimac, A. K. (1999). Standup and stabilization of the inverted pendulum (Doctoral dissertation, Massachusetts Institute of Technology, Dept. of Mechanical Engineering).